CALCULATION OF RIP CURRENTS USING A THREE-DIMENSIONAL NEARSHORE CURRENTS MODEL

Jeho Chun[1], Kyungmo Ahn[2], Kyung-Duck Suh[3], Tae-Soon Kang[4]

Abstract

In the present study, we have applied the three-dimensional nearshore currents model considering the wave-current interaction to calculate the rip currents at Haller et al.'s (2000) hydraulic experiment and Haeundae beach. In order to see the effect of wave-current interaction on the rip currents, the numerical simulations without the wave-current interaction have been also carried out. Two numerical results show that the accuracy of the numerical simulation with the wave-current interaction is higher than the other, because the wave fields of the numerical results with the wave-current interaction were more accurately calculated. Especially, the computed rip currents speeds at Haeundae beach were closer to the measured rip currents, if the tidal currents were considered in the numerical simulation.

Key words: Rip-currents, Wave-current interaction, Three-dimensional nearshore currents model, Haller's (2000) experiment, Haeundae beach

1. Introduction

The rip currents are water jet issuing through the breaker line (Dean and Dalrymple, 2002). Since it causes the marine accidents at the beach, or it moves sand particles to the offshore, a lot of studies have been carried out (Dalrymple et al., 2010; Droenen and Deiggard, 2007; Haas et al., 2003; Haas and Warner, 2009; Haller et al., 2000). Even though major driving forces of the rip currents are the surface waves, the non-uniformly distributed wae breakng energy in the along shore direction by the bottom topography and oceanographic conditions such as tides and tidal currents give a major influence on the generation of the rip currents. Owing to its complexity of rip currents, they are usually calculated by the numerical models.

The high-order nonlinear wave models and long wave equation with radiation stresses are used to calculate the rip currents. In the high-order nonlinear wave models, Boussinesq wave model or non-hydrostatic wave model is used for the computation of rip currents (Chen et al., 1999; Choi et al., 2011; Jacobs, 2010). The high-order nonlinear wave models accurately compute both of surface waves and rip currents. Especially, these models can successfully calculate the low frequency waves as well. However, it is difficult to consider the oceanographic conditions of tides and tidal currents, even though the effects of tides are very important in several cases (Dalrymple et al., 2010; Kim et al., 2011).

Whereas the long wave equation does not provide both of the wave fields and nearshore currents fields, it take into consideration the various factors such as tides and tidal currents for the computation of rip currents. Recently, quasi-three-dimensional or three-dimensional nearshore currents model is used to calculate the nearshore currents fields (Haas et al., 2003; Haas and Warner, 2009; Mellor, 2003; Newberger and Allen, 2007). The three-dimensional nearshore currents model is advantageous to obtain

[1]Senior engineer, Department of Coastal Management, Geosystem Research Corporation, Hanlim Human Tower, 1-40, Geumjeong-Dong, Gunpo-si, Geyonggi-Do, Republic of Korea, eulia01@hotmail.com
[2]Professor, School of Spatial Environmental System Engineering, Handong Global University, Heunghae-eup, Buk-gu, Pohang, Gyeongbuk, Republic of Korea, kmahn@handong.edu
[3]Professor, Department of Civil and Environmental Engineering, Seoul National University, 1 Gwanak-ro, Gwanak-gu, Seoul 151-744, Republic of Korea, kdsuh@snu.ac.kr
[4]Director, Department of Coastal Management, Geosystem Research Corporation, Hanlim Human Tower, 1-40, Geumjeong-Dong, Gunpo-si, Geyonggi-Do, Republic of Korea, kangts@geosr.com

both of the depth-averaged nearshore currents fields and the velocity profiles of nearshore currents.

In the present study, a three-dimensional nearshore currents model within the Eulerian framework was used to calculate the rip currents, which was dynamically coupled with the wave model. In this numerical model, the surface stress considering the surface waves and wave-induced Reynolds stress were incorporated (Chun, 2012). For its verification, this numerical model have been applied to the several experimental problems on the longshore currents, rip currents, and undertow.

2. Nearshore Currents Model

The present neashore currents model was developed to calculate the three-dimensional nearshore currents (Chun, 2012). For the computation of three-dimensional nearshore currents, the sigma coordinate was employed in the vertical grid of present numerical model. The momentum equation of present numerical model is the same as that of De Vriend and Stive (1987) and Svendsen and Lorenz (1989). But, the present numerical model is different from their numerical models in the points that new surface stress and wave-induced Reynolds stress were employed to the present numerical model. In the present paper, the formulations of surface stress and wave-induced Reynolds in the x-direction are given as

$$\begin{aligned}\tau_{\bar{\eta},x} = &\left[M_y \left(\frac{\partial V}{\partial x} - \frac{\partial U}{\partial y} + f \right) + D \frac{\partial}{\partial x} \left(\frac{Ek}{\sinh 2kD} \right) + \frac{D_{br} k_x}{\omega_r} \right] \\ &+ \left(\frac{\partial S_{xx}}{\partial x} + \frac{\partial S_{xy}}{\partial y} \right) - \left(\frac{1}{2} \frac{\partial E}{\partial x} - \rho \left\langle \tilde{w}_{\bar{\eta}}^2 \right\rangle \frac{\partial \bar{\eta}}{\partial x} \right) + \tau_{s,x}\end{aligned} \tag{1}$$

$$\left\langle \tilde{u}\tilde{w} \right\rangle = \left\langle \tilde{u}^2 \right\rangle \left(\frac{\partial \bar{\eta}}{\partial x} + \sigma \frac{\partial D}{\partial x} \right) + \left\langle \tilde{u}\tilde{v} \right\rangle \left(\frac{\partial \bar{\eta}}{\partial y} + \sigma \frac{\partial D}{\partial y} \right) \tag{2}$$

The details of numerical model are given in Chun (2012). The depth-integrated form of present numerical is the equivalent with that of numerical model of Smith (2006) and Newberger and Allen (2007)

3. Haller et al.'s (2000) experiment

Haller et al.'s (2000) conducted the hydraulic experiments for the rip currents in a three-dimensional wave basin, where three sand bars with gaps were located on the sloping bottom (1:30) as shown in Figure 1. In this hydraulic experiment, the typical rip currents such as shoreward flows over the sand bars and seaward return flows at the rip channels were observed, and additionally the low frequency waves were also generated. These rip currents were numerically reproduced by Kumar et al. (2011), Haas et al. (2003) and Haas and Warner (2009).

Haas et al. (2003) have applied the SHORECIRC model to the test case B of this experiment. Through the numerical study, they have investigated the characteristics of rip currents on the experiment. The accuracy of their numerical results was quantified by the index of agreement

$$d = 1 - \frac{\sum_{i=1}^{n} \left(x_m - x_c \right)^2}{\sum_{i=1}^{n} \left(\left| x_m - \overline{x}_m \right| + \left| x_c - \overline{x}_m \right| \right)^2} \tag{3}$$

where x_m and x_c represent the measured and computed values, respectively, and $\overline{x}_m$ is the mean value of the measurements. In the numerical results of Haas et al. (2003), the values of the index of

agreement for mean water levels, longshore currents, and cross-shore currents are 0.96, 0.92, and 0.80, respectively. And it is remarkable that the low-frequency wave and longshore currents in front of the middle sand bar were also successfully reproduced in their numerical simulation. We have also applied our numerical model to the same case as Haas et al. (2003), test case B. In the present numerical simulation, the incident wave height and period are given as 5.12 cm and 1.0 s, respectively. The spatial grid size is 0.2 m. Time step and model time are given as 0.1 s and 300 s, respectively. As the offshore boundary condition for the mean water level, the following equation is used.

$$\overline{\eta} = -\frac{H^2 k}{8 \sinh 2kh} \tag{4}$$

The Eq. (4) was derived by the Bernoulli equation (Dean and Dalrymple, 1991). And it is also employed at the offshore boundary condition of wave set-up module of SBEACH (Larson and Kraus, 1989). Along with the measurements, the numerical results are presented in Figure 3 ~ Figure 7. In these figures, the numerical results for the case without the wave-current interaction are also included.

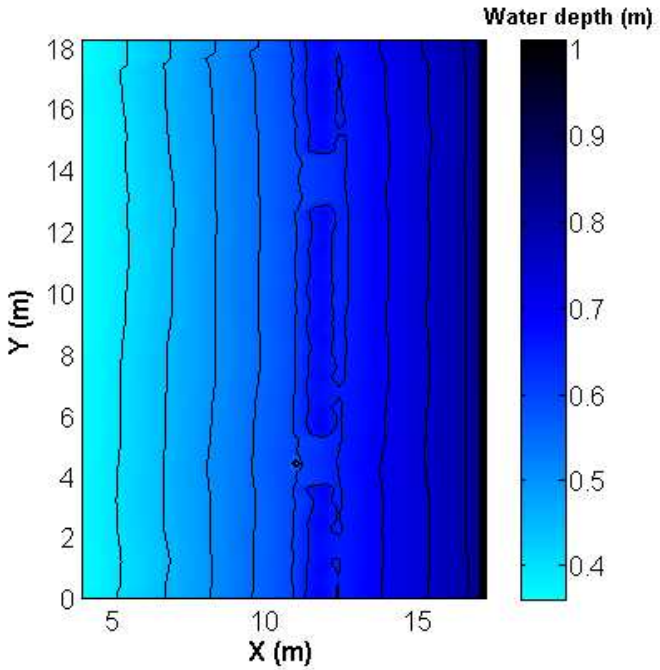

Figure 1. Bottom topography for Haller et al. (2000) experiment.

With the measurements, the computed wave heights in the direction along and across the shoreline are presented in Figure 2 and Figure 3, respectively. These figures show that the computed wave heights well agree with the measured ones. Of two cases, the computed wave heights considering the wave-current interaction are more accurate. It is also shown in the statistical quantities such as bias, RMSE, SI, and r . In the computed wave heights with the wave-current interaction, bias, RMSE, SI, and r are 0.0056 cm, 0.92 cm, 0.19, and 0.88, respectively. Meanwhile, the model accuracy for the case without the wave-current interaction is a little lower than that with the wave-current interaction, although they are much different in Figure 2 and Figure 3. The bias, RMSE, SI and r are -0.0052 cm, 1.11 cm, 0.20, and 0.87. The differences between two computed wave heights are obviously shown at the points around the sand bars and rip channels, as shown in Figure 3. Even though the wave breaking occurred in both of cases, the

following currents on the sand bars reduced the wave heights. Due to the action of the currents on the waves, the wave heights for the coupled case become more accurate. These rip currents have also influenced the distributions of wave heights at the rip channel. As shown in Figure 3(b), the wave heights for the coupled case are a little larger than that without the wave-current interaction owing to the opposing currents. In Figure 3(b), the wave heights for the decoupled case are more accurate. However, the accuracy in the wave heights for the coupled case is higher than the other case.

The differences in the distribution of wave heights lead induce the differently distributed wave breaking energy, as shown in Figure 4. For both of cases, the strength and position of wave breaking energy are different each other. Due to the small water depth on the sand bars, the position of wave breaking for both of cases is the same. However, the wave breaking energy for the decoupled case is much larger than that for the coupled case, because the wave heights for the coupled case are lower than the other case owing to the following currents on the sand bars. Meanwhile, the magnitudes of wave breaking energy at the rip channels for both of cases are similar each other, but the positions of wave breaking are different each other due to the shortened wave lengths by the opposing currents. The differences in the wave breaking energy and wave heights give an influence on the mean water levels and depth-averaged nearshore currents.

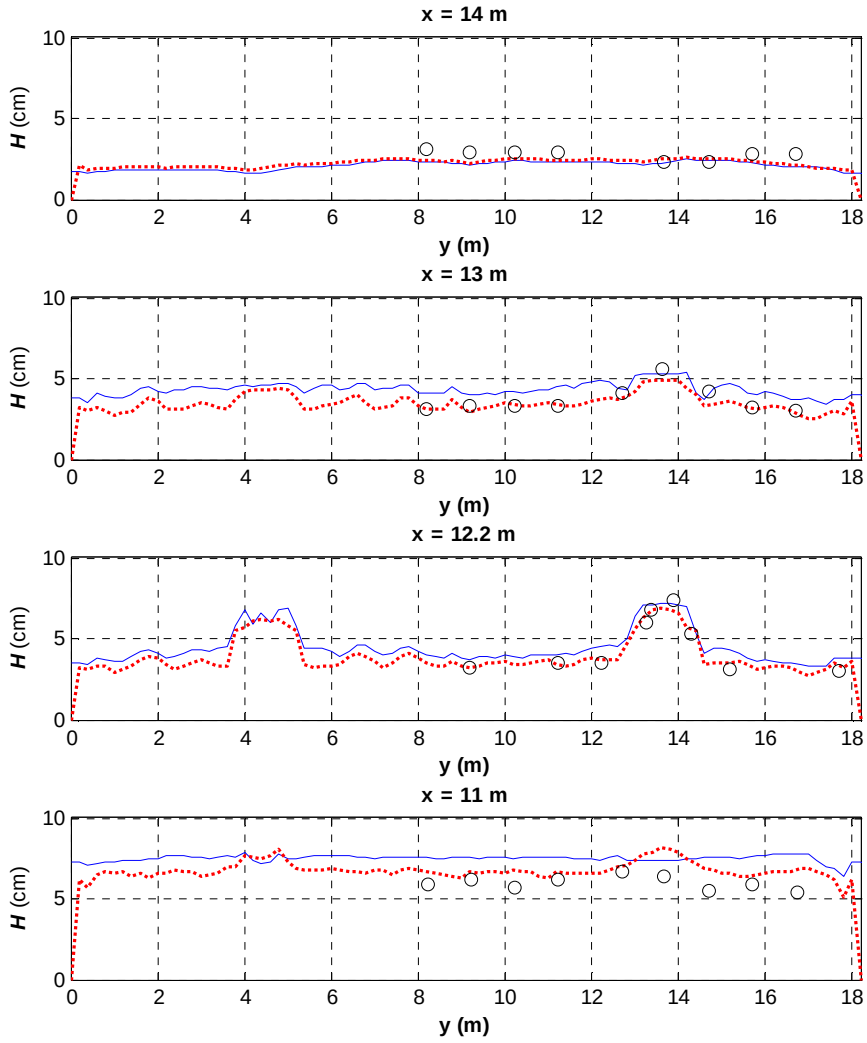

Figure 2. Comparison of the wave heights at x = 10 m, 11 m, 12.2 m, 13 m, 14 m : the measured wave heights (circle); numerical results for the decoupled case (solid line); numerical results for the coupled case (dotted line).

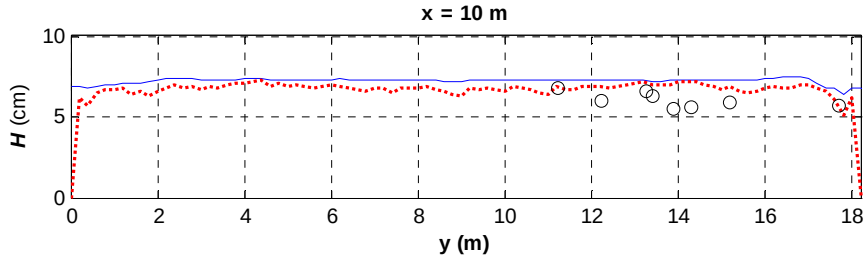

Figure 2. Continued

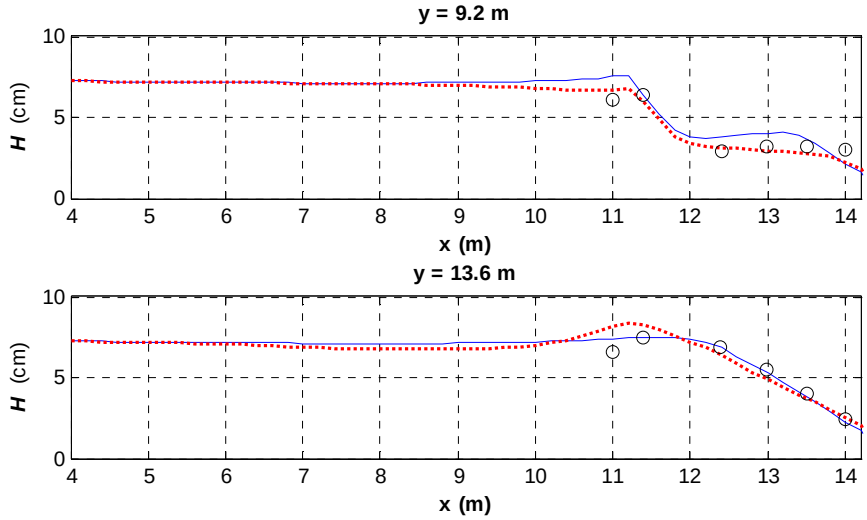

Figure 3. Comparison of the wave heights at y = 9.6 m, 13.6 m : the measured wave heights (circle); numerical results for the decoupled case (solid line); numerical results for the coupled case (dotted line).

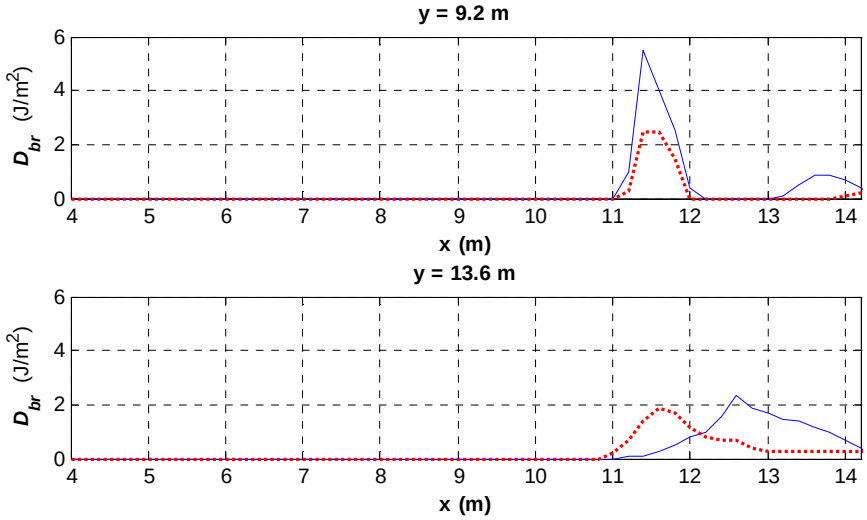

Figure 4. Comparison between the wave breaking energy for the decouple case (solid line) and one of the coupled case (dotted line).

The computed and measured mean water levels are presented in Figure 5. The typical mean water levels in the rip channel are shown: the relatively higher mean water levels on the sand bars; the wave set-

up at the shoreline; the wave set-down at the wave breaking points. Although there are a little underestimation in the computed mean water level at x = 10 m and 11 m, the computed mean water levels for the coupled case well agree with the measurements. On the other hand, the mean water levels for the decoupled case are largely overpredicted owing to the larger wave breaking energy at the sand bars, which are shown in Figure 4. This overprediction is also shown in Figure 7.

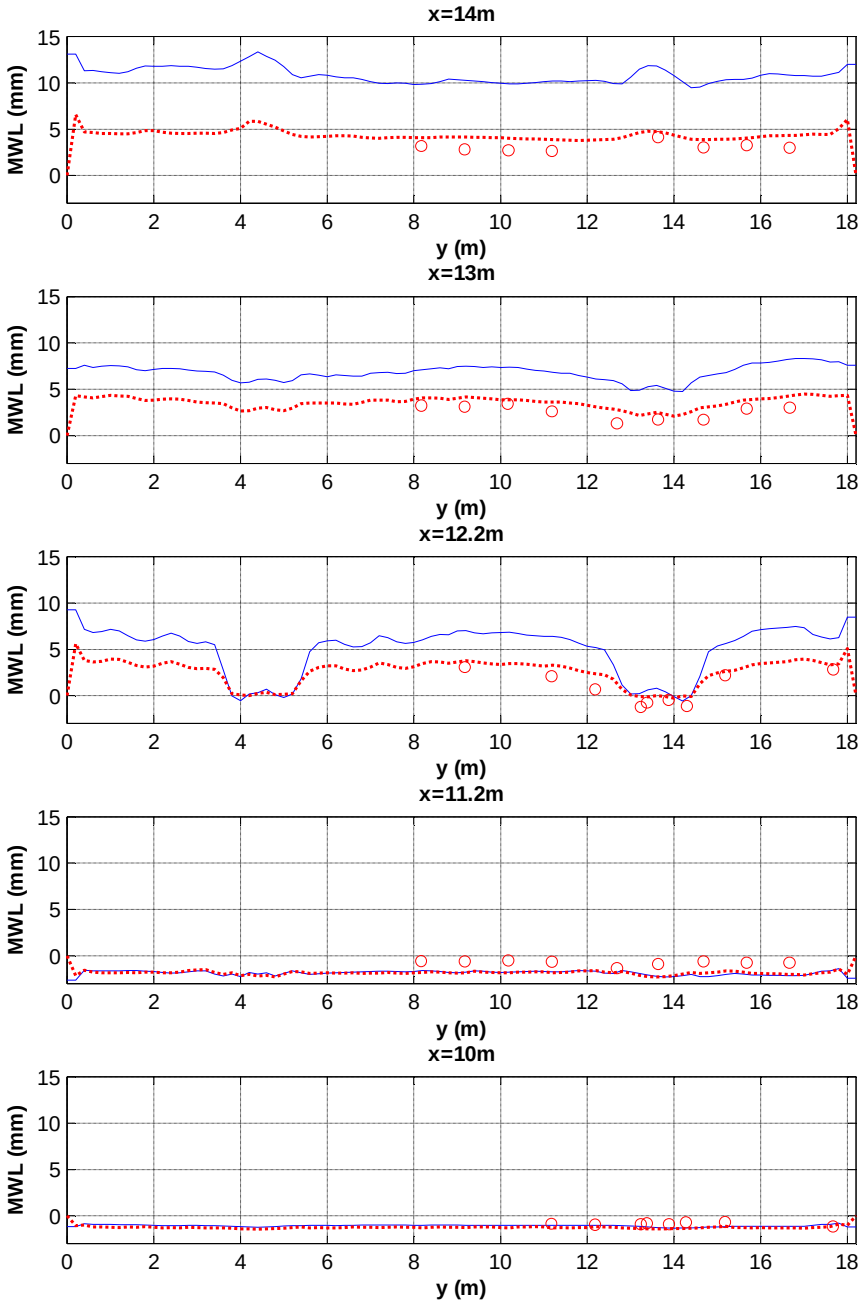

Figure 5. Comparison of the mean water levels at x = 10 m, 11 m, 12.2 m, 13 m, 14 m : the measured mean water levels (circle); numerical results for the decoupled case (solid line); numerical results for the coupled case (dotted line).

Along with the measured ones, the computed longshore and cross-shore currents are presented in Figure 6 and Figure 7, respectively. In these figures, the typical rip currents such as the rip feeder at the shore-side

of sand bars, shoreward flows on the sand bars and the return flows at the rip channels are reproduced. Although the cross-shore currents on the sand bars have some irregular pattern due to the irregular bottom topography, there are good agreements between the measured and computed ones. The depth-averaged velocities were also overestimated, if the wave-current interaction was not considered. Especially, the calculated cross-shore currents at the rip channel were much larger than the measured ones. It was also reflected in the quantitative assessments of numerical models. In this case, the indices of agreement of mean water levels, longshore currents, and cross-shore currents are 0.69, 0.91 and 0.82, respectively. On the other hand, the indices of agreements for the mean water levels, longshore currents, and cross-shore currents for the coupled case are 0.97, 0.94 and 0.90, respectively.

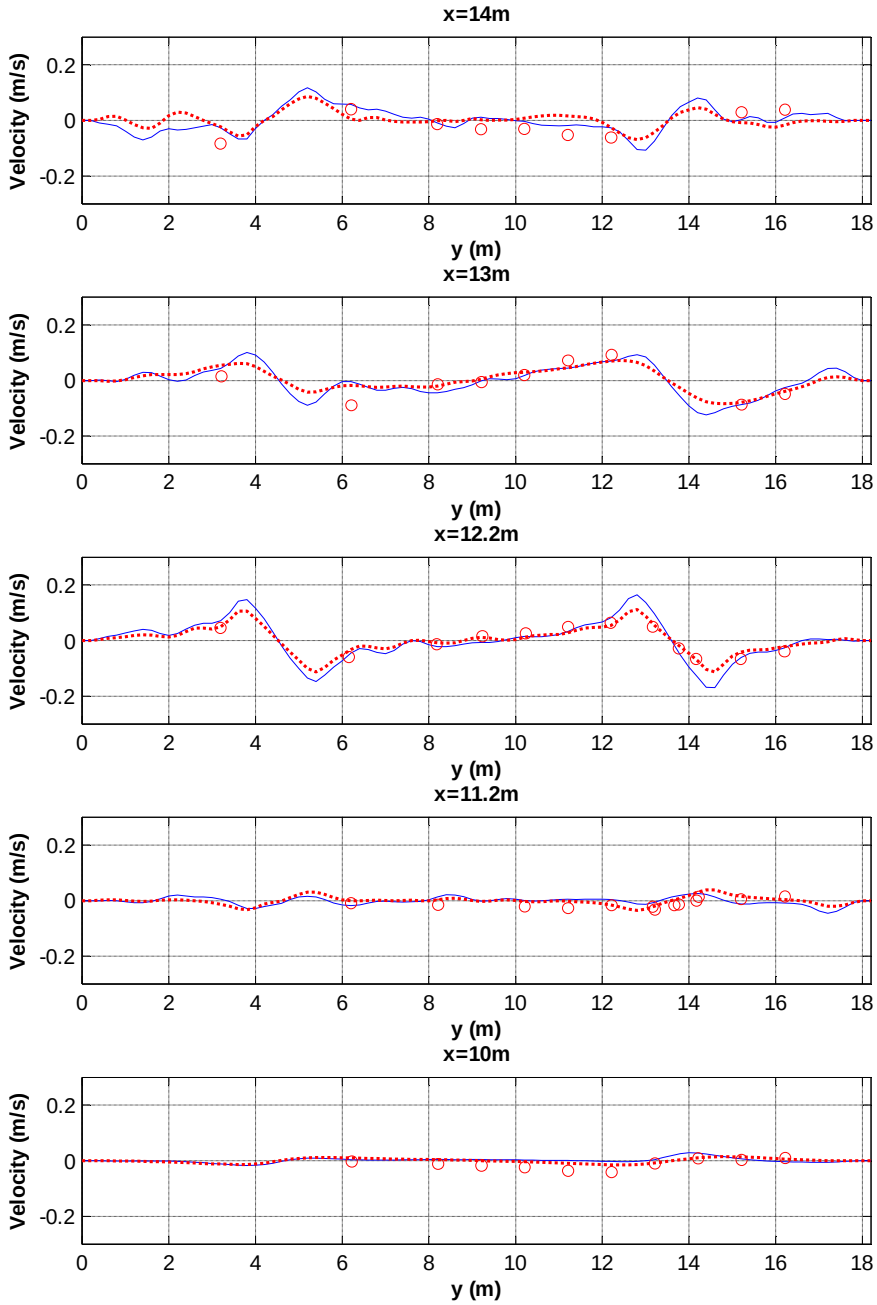

Figure 6. Comparison of the depth-averaged longshore currents at x = 10 m, 11 m, 12.2 m, 13 m, 14 m : the measured depth-averaged longshore currents (circle); numerical results for the decoupled case (solid line); numerical results for the coupled case (dotted line).

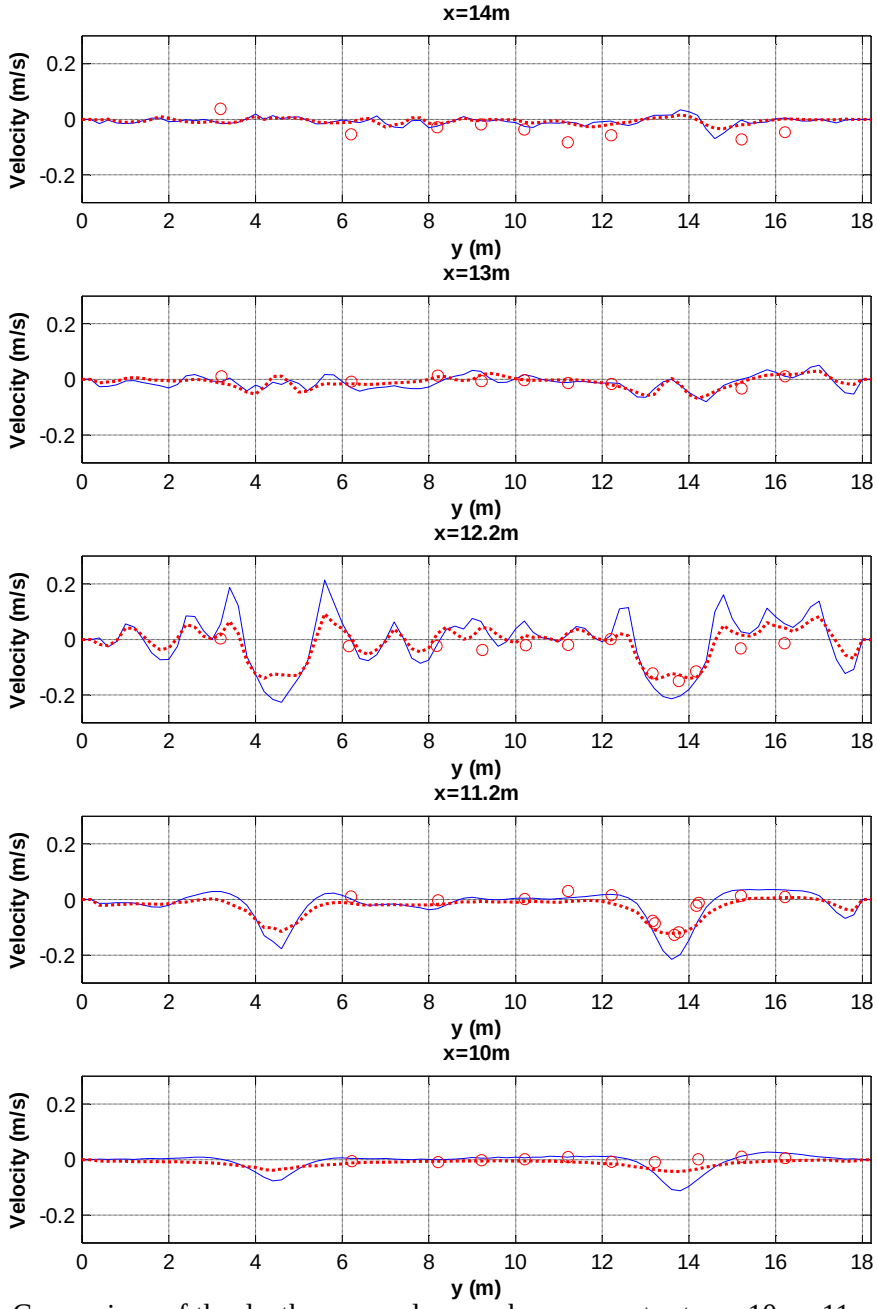

Figure 7. Comparison of the depth-averaged cross-shore currents at x = 10 m, 11 m, 12.2 m, 13 m, 14 m : the measured depth-averaged cross-shore currents(circles); numerical results for the coupled case (solid line); numerical results for decoupled case (dotted lines)

4. Rip Currents in Haeundae Beach

On 8th July 2010, the rip currents with a speed of 0.3 m/s were measured at Haeundae beach. At that time, the incident wave condition was given as H_s = 0.9 m, T_p = 11.2 s, and θ_m = 216° from the wave hindcasting of KMA (Korean Meteorological Administration). Likewise the most of marine accidents by rip currents, the wave energy was not high. However, the water level was on high tide condition, and even the rip currents were obliquely incident to the beach. This condition is uncommon, but the rip currents at Truc Vert, France, were also observed in the high tide condition (Dalrymple et al., 2010). Actually, Kim reports that the most of rip currents at Haeundae beach were observed near the high tide level. It implies

that the tidal current and tidal level crucially give an effect on the generation of rip currents at Haeundae beach. In this section, the importance of tide condition in the generation of rip currents at Haeundae beach was shown by performing the numerical simulations with and without the tide and tidal currents.

The bottom topography at Haeundae beach was presented in Figure 8. As shown in Figure 8, it is difficult to find the bathymetric variations at the shorefaces of Haeundae beach, even though there are several shoals at the offshore region of Haeundae beach. Due to this complex bottom topography, the weak rip currents were calculated. In this numerical simulation, uni-directional random wave was considered as the incident wave condition. The spectral form of incident wave was defined as the most probable wave spectrum in Haeundae beach. Without the tidal conditions, the calculated rip currents speeds at Haeundae beach was just half of the measured ones, 0.18 m/s. Although the bottom topography near Haeundae beach are complicated, the incident waves were obliquely incident to the study area. It leads to the weak rip currents.

Considering the tidal conditions, we have conducted a numerical simulation for the tidal currents at first. From this tide model, the tidal boundary condition for the computation of rip currents was obtained. The present tide model was validated by comparing the computed tidal elevations with the predicted ones. The bias, RMSE, SI, and r of the present tide model were 0.01 cm, 7.67 cm, -81.593, and 0.96, respectively. The tidal currents at the accidents time are presented in Figure 9. The tidal currents flow eastward, and the anti-clockwise circular flow is shown in front of Haeundae beach. The tidal currents speed at the points was 9 cm/s, where the rip currents were generated. Even though the tidal currents speeds were small, the tidal currents influenced on the wave fields propagating over the complex bottom topography. It intensified the non-uniformity in the spatial distribution of wave breaking energy in front of Haeundae beach.

The depth-averaged nearshore current velocities without the tidal currents are presented in Figure 10. The current measurement point is presented by the circle. In this case, the rip current speed at the measurement point is are 0.18 m/s. It is just a half of the measured rip currents speed. The depth-averaged nearshore current velocities with the tide condition are presented in Figure 11. But, the currents speeds in Figure 11 are larger than those without the tidal boundary conditions owing to the tidal currents velocity. As shown in Figure 11, the rip currents appear more obviously, because wave heights are increased by the ebb currents. In this case, the rip current speed at the measurement point is 0.3805 m/s. In the present section, it is concluded that the tidal boundary condition should be contained in the generation of rip currents at Haeundae beach.

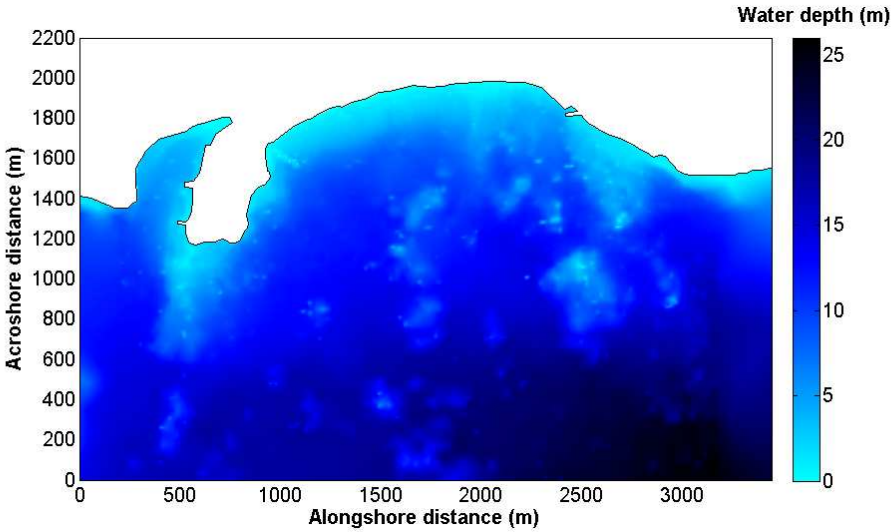

Figure 8. Bottom topography of Haeundae beach.

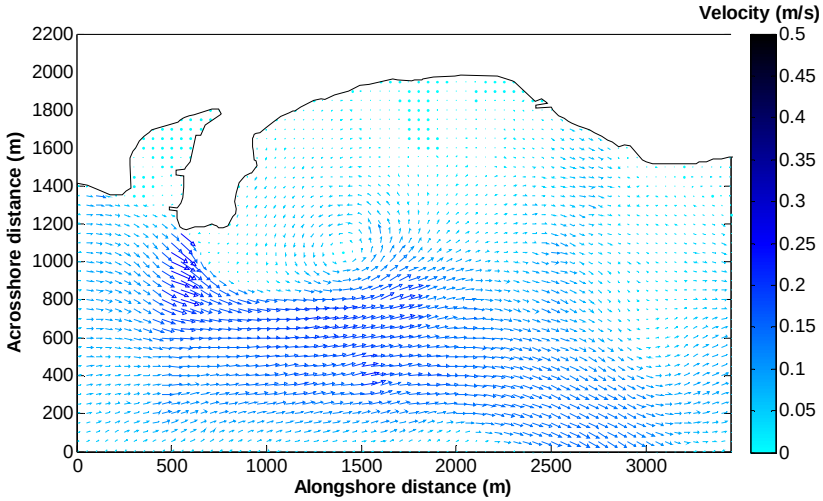

Figure 9. The velocity vector of tidal currents at the time of marine accident by rip currents.

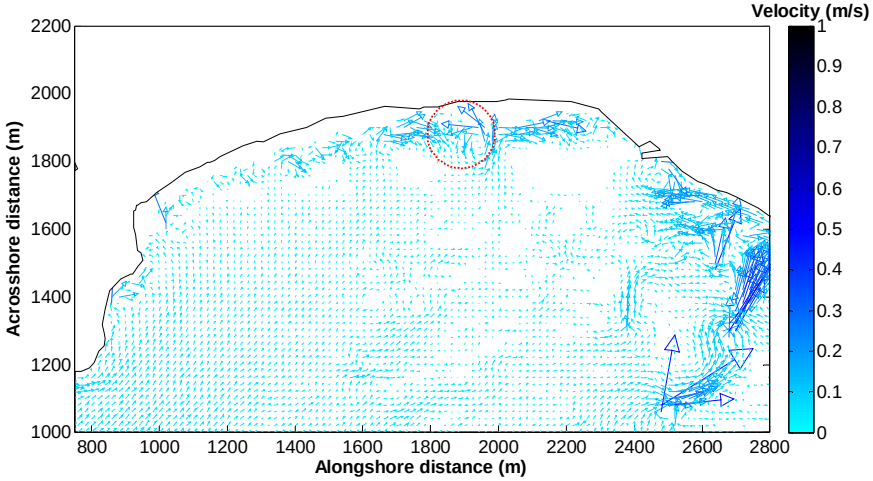

Figure 10. Depth-averaged current velocity at Haeundae beach, the case without the tidal currents.

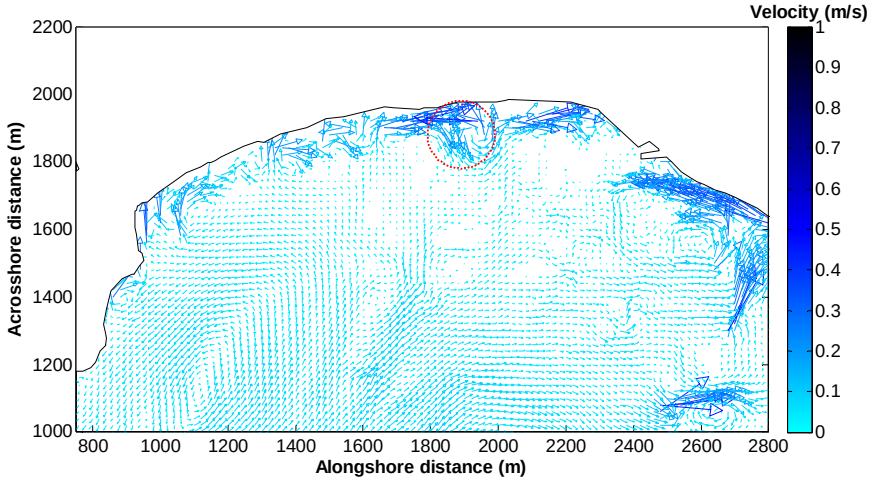

Figure 11. Depth-averaged current velocity at Haeundae beach the case with tidal currents.

5. Conclusions

In most of cases, the non-uniform distribution of wave breaking energy in the alongshore direction induces the rip currents. Usually, this non-uniformity is resulted from the bottom topography, but the rip currents and tidal currents also influence on that. Therefore, the wave-current interaction should be considered for the accurate computation of rip currents. In the present study, we have shown its significance by performing the numerical simulations with and without the wave-current interaction. In the present numerical simulations, the three-dimensional nearshore currents model considering wave-current interaction was employed. This numerical model was developed in Eulerian framework, and it is different from that of Newberger and Allen (2007) in the point that this model does not assume the shallow water wave conditions.

In the present numerical simulation, the numerical results with the wave-current interaction were more accurate than that without it. In Haller et al.'s (2000) hydraulic experiment, the wave breaking energy was overestimated in the case without the wave-current interaction, and then the overestimated wave breaking energy leads to the overprediction in mean water levels, and depth-averaged velocities. Meanwhile, the rip currents at Haeundae beach was underestimated, if the wave-current interaction was not considered. Although the tidal currents speeds was not large, it influenced on the wave fields, and it leads to underprediction of rip currents. Throughout two numerical simulations, it is concluded that the wave-current interaction is important to calculate the rip currents.

Acknowledgements
This study was supported by a grant 'Development of countermeasure techniques against large swells using IT' [NEMA-NH-2011-43] from the Natural Hazard Mitigation Research Group, National Emergency Management Agency of Korea.

References

Chen, Q., Dalrymple, R.A., Kirby, J.T., Kennedy, A.B. and Haller, M.C., 1999. Boussinesq modeling of a rip current system. *Journal of Geophysical Research*, 104(c9): 20,617 ~ 20,637.

Choi, J., Park, W.K. and Yoon, S.B., 2011. Boussinesq modeling of a rip current at haeundae beach. *Journal of the Korean Society of Coastal and Ocean Engineers*, 23(4): 276 ~ 284 (in Korean).

Chun, J., 2012. *3d numerical model of nearshore currents considering wave-current interaction*. Ph.D Thesis, Seoul National University.

Dalrymple, R.A., MacMahan, J.H., Reniers, A.J.H.M. and Nelko, V., 2010. Rip currents. *Annual Review In Fluid Mechanics*, 43: 551 ~ 581.

Dean, R.G. and Dalrymple, R.A., 1991. *Water wave mechanics for engineers and scientists*. World Scientific Publishing, Co. Pte. Ltd.

Dean, R.G. and Dalrymple, R.A., 2002. *Coastal processes with engineering applications*. Cambridge University Press.

De Vriend, H.J., and Stive, M.J.F., 1987, *Quasi-3D modeling of nearshore currents.* Coastal Engineering 11: 565 ~ 601.

Droenen, N. and Deiggard, R., 2007. Quasi-three-dimensional modeling of the morphology of longshore bars. *Coastal Engineering*, 54: 197 ~ 215.

Haas, K.A., Svendsen, I.A., Haller, M.C. and Zhao, Q., 2003. Quasi-three-dimensional modeling of rip current system. *Journal of Geophysical Research*, 108(c7): doi:10.1029/2002JC001355.

Haas, K.A. and Warner, J.C., 2009. Comparing a quasi-3d to full 3d nearshore circulation model: Shorecirc and roms. *Ocean Modeling*, 26: 91 ~ 103.

Haller, M.C., Dalrymple, R.A. and Svendsen, I.A., 2000. *Experiments on rip currents and nearshore circulation: Data report, research report, cacr-00-04* Center for Applied Coastal Research, Ocean Engineering Laboratory, University of Delaware.

Jacobs, R.P.M., 2010. *Non-hydrostatic computations of nearshore hydrodynamics*, Delft university of technology.

Kim, I.H., Kim, I.C. and Lee, J.L., 2011. Rip current prediction system combined with a morphological change model. *Journal of Coastal Research*, Special issue 64: 547 ~ 551.

Larson, M. and Kraus, N.C., 1989. *Sbeach: Numerical model for simulating storm-induced beach change; report 1: Empirical foundation and model development*, U.S. Army Corps of Engineers Engineer Research and Development Center.

Mellor, G.L., 2003. *Users guide for a three-dimensional, primitive equation, numerical ocean model*, Prog. in Atmos. an Ocean Sci., Princeton University.

Newberger, P.A. and Allen, J.S., 2007. Forcing a three-dimensional, hydrostatic, primitive-equation model for application in the surf zone : 1. Formulation. *Journal of Geophysical Research*, 112: C08018, doi:10.1029/2006JC003472.

Svendsen, I.A. and Lorenz, R.S. 1989. *Velocities in combined undertow and longshore currents.* Coastal Engineering 13: 55 ~79.